Int. J. Electrochem. Sci., 12 **(2017)** 7197 – 7204, doi: 10.20964/2017.08.53

International Journal of
ELECTROCHEMICAL
SCIENCE
www.electrochemsci.org

Short Communication

Synthesis of Fe_3O_4 Nanorings/Amine-Functionalized Reduced Graphene Oxide Composites as Supercapacitor Electrode Materials in Neutral Electrolyte

Fanghua Zhu[1], *Yuguang Wang*[1,*], *Yunwang Zhang*[1], *Wei Wang*[2]

[1] Research Center of Laser Fusion, China Academy of Engineering Physics, Mianyang, Sichuan 621900, China.
[2] School of Materials Science and Engineering, Southwest University of Science and Technology, Mianyang, 621010, China
[*]E-mail: ygwang1228@163.com

Received: 8 November 2016 / *Accepted:* 6 June 2017 / *Published:* 12 July 2017

Fe_3O_4 supported on nitrogen-doped graphene was prepared by a facial one-pot hydrothermal method. The cyclic voltammetry, constant current charge and discharge, AC impedance and cycle times were tested in 1.0 mol/L Na_2SO_4 aqueous solution. The results of electrochemical measurements show that the Fe_3O_4 nanorings (NRs)/amine modified reduced grapheme oxide (NH_2-RGO) composites have high capacitance, good conductivity, excellent ion diffusion behavior and strong stability. In neutral electrolyte, the specific capacitance measured under the current condition of 1.0 A/g was as high as 145 F/g, and the capacitance retention after the 1000-cycle constant-current charge-discharge test was 99.7%. Therefore, Fe_3O_4 NRs/NH_2-RGO composites have a good prospect as supercapacitor electrodes.

Keywords: Fe_3O_4 Nanorings, Supercapacitor, Graphene, Electrode material

1. INTRODUCTION

Supercapacitor is also called electrochemical capacitor, which is an energy storage device between battery and traditional capacitor [1,2]. Supercapacitor has higher energy density than traditional capacitor and the larger power density than battery. In recent years, supercapacitor has been widely utilized in the fields of new energy power generation, electric vehicle, national defense science and technology, aviation and spaceflight [3-5].

In general, supercapacitors can be classified as electrical double layer capacitors (EDLCs) and pseudocapacitors [6,7]. EDLCs, such as carbon-based materials, can provide a longer cycle life but qwrfdewrlower specific capacitance, leading to the rather low energy density and power density [8,9]. Compared with EDLCs, pseudocapacitors, such as metal oxides/hydroxides, show higher specific capacity and energy density, but poor reversibility [10-12]. Therefore, we need to combine these two charge storage mechanisms, and design composite materials. The composite materials would exhibit synergistic effects of EDLCs and pseudocapacitors, expected to become an ideal electrode material for supercapacitor.

Recently, many researchers have been focused on transition metal oxides/carbon-based composites as electrode materials due to their high specific capacitance, high energy density and excellent reversibility [8,13,14]. Among these transition metal oxides, Fe_3O_4 has the advantages of low cost, abundant natural resources and low environmental pollution, is considered to be a superior pseudocapacitive material and ideal electrode materials for supercapacitor [15-19].

Li *et al.*[20] prepared 5 nm Fe_3O_4 nanoparticles grown on reduced graphene oxide (Fe_3O_4/rGO), and the electrode material possesses a high specific capacitance of 241 F/g at 1.0 A/g within the potential range from -1 to 0 V and an excellent cycling stability of 79.2% after 1000 cycles at a high current density of 10 A/g. Liu *et al.*[21] prepared carbon-coated Fe_3O_4 nanorods via hydrothermal reaction. And these carbon-coated Fe_3O_4 (Fe_3O_4/C) nanorods present improved electrochemical performance with a specific capacitance of 275.9 F/g at a current density of 0.5 A/g in 1.0 M Na_2SO_3 aqueous solution.

In this paper, we show a facile and efficient method to prepare Fe_3O_4 nanorings (NRs)/amine modified reduced grapheme oxide (NH_2-RGO) composites, and utilized them as advanced supercapacitor electrode materials. The Fe_3O_4 NRs/NH_2-RGO electrode material exhibits positive synergistic effects of pseudocapacitance and EDLC between Fe_3O_4 NRs and NH_2-RGO, leading to high specific capacitance and excellent reversibility in neutral electrolyte. The Fe_3O_4 NRs/NH_2-RGO electrode material possesses specific capacitance of 145 F/g at 1.0 A/g in 1.0 M Na_2SO_4 electrolyte solution. Moreover, the electrode material exhibits an excellent cycling stability of 99.7 % after 1000 cycles at a high current density of 1.0 A/g. These results show that such synthetic method may open a new route to design safe and cost-effective electrochemical supercapacitors.

2. EXPERIMENTAL

2.1 Materials

Graphite powder (99.95%, 8000 mesh) was purchased from Shanghai Aladdin Reagent Company. H_2SO_4 (98%), HCl, HNO_3, potassium persulfate, phosphorus pentoxide, acetone, ethanol, ammonium persulfate, aniline, $KMnO_4$, $Ba(NO_3)_2$ and hydrazine hydrate were purchased from Chengdu Kelon Chemical Reagent Company. Perchloric acid (analytical grade) and H_2O_2 (30%) were purchased from Tianjin Zhengcheng Chemical Products Co., Ltd. The water used in the experiment was distilled water.

2.2 Preparation of Fe_3O_4 NRs/NH_2-RGO

Firstly, the uniform Fe_3O_4 NRs were prepared by a hydrothermal method according to *Jia et al*. [22]. GO was synthesized by modified Hummers method as described in the previous studies [23,24]. In a typical experiment, 1.0 mg of Fe_3O_4 NRs was dispersed in 5.0 mL of dimethyl formamide (DMF), and then the suspension was prepared by ultrasonic dispersion for 30 min. Subsequently, 100 mg of GO was weighed into 40 mL of ethylene glycol and dispersed ultrasonically for 5 hours. The supernatant was separated by centrifugation and 1.0 mL of aqueous ammonia was added. The mixture was transferred to a reaction vessel of polytetrafluoroethylene and reacted at 180 °C for 12 h. Finally, the target product after the reaction was washed with distilled water and freeze-dried to obtain an NH_2-RGO nanometer matrix.

2.3 Characterization

The morphology and microstructure of the products were characterized by field emission scanning electron microscopy (FSEM, Ultra 55) and transmission electron microscopy (TEM, 200FE Libra). Electrochemical results were obtained using a German IM6 electrochemical workstation.

The sample, acetylene black and polytetrafluoroethylene were uniformly mixed at a ratio of 80:15:5. After the ultrasonic dispersion, the composite material in the form of paste was coated on the stainless steel collector and pressed at a pressure of 10 M Pa, and dried to the same quality. The electrode was platinum electrode, the reference electrode was saturated calomel electrode, and the working electrode was the stainless steel net collector with constant mass. The electrolyte was 1.0 mol/L Na_2SO_4 solution. The working electrode was subjected to cyclic voltammetry (CV), constant current charging and discharging and AC impedance test.

3. RESULTS AND DISCUSSION

3.1. SEM measurement

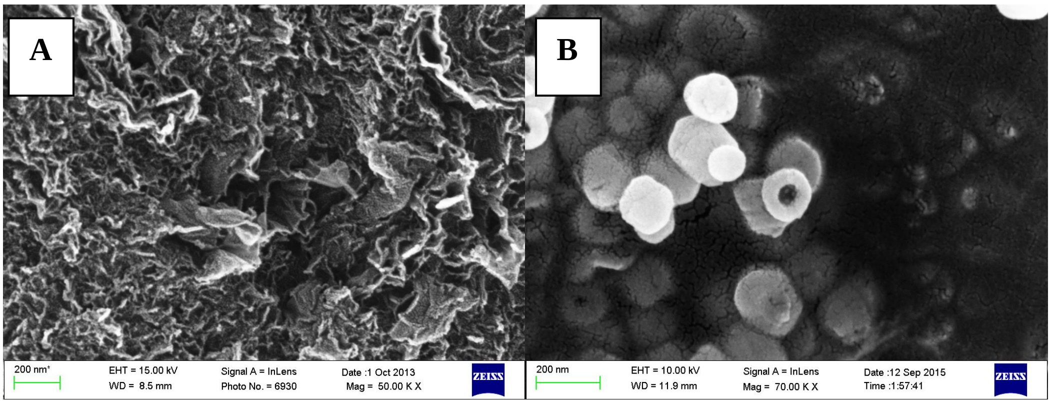

Figure 1. SEM images of NH_2-RGO (A) and Fe_3O_4 NPs/ NH_2-RGO composites (B).

The SEM images of NH_2-RGO (A) and Fe_3O_4 NRs/NH_2-RGO composites (B) are shown in Figure 1. It can be seen that NH_2-RGO nanomaterials are mainly composed of randomly thin lamellar layers and form a porous and disordered network structure. This morphology favors contact of the electrolyte with the surface of the Fe_3O_4 NPs/NH_2-RGO composites.

3.2 CV curves

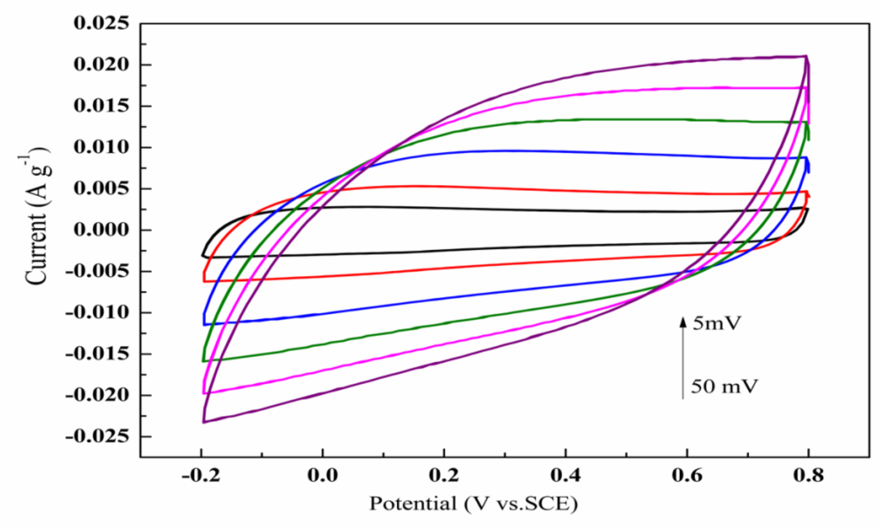

Figure 2. CV curves of Fe_3O_4 NRs/NH_2-RGO electrode at different scanning rates.

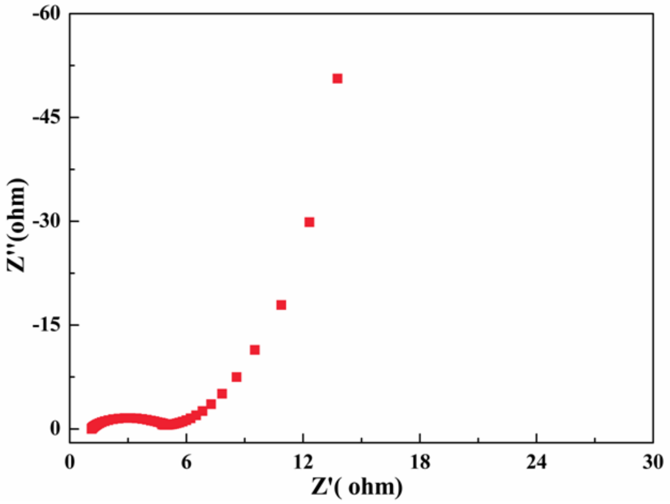

Figure 3. The Niquist plots of Fe_3O_4 NRs/NH_2-RGO electrode.

The cyclic voltammetric curves of Fe_3O_4 NRs/NH_2-RGO composites in 1.0 mol/L Na_2SO_4 solution are shown in Figure 2. The potential test window is -0.2~0.8V. The CV curves of the Fe_3O_4 NRs/NH_2-RGO composites electrode are close to the rectangular shape and have no redox peak, which shows the electric double layer capacitance characteristic. The CV curves of the Fe_3O_4 NRs/NH_2-RGO composites remain essentially constant as the scanning rate increases. As the scanning rate increases, the response current increases as well, mainly because the size of the current is proportional to the mass transfer rate when the electrochemical process is diffusion controlled during the CV test. In addition, these CV curves remain similar in shape and the current response increases with a scan rate from 5 to 50 mV/s, indicating that the Fe_3O_4 NRs/NH_2-RGO composites is beneficial for rapid and reversible redox reactions [25].

The AC impedance spectra of Fe_3O_4 NRs/NH_2-RGO composites are shown in Figure 3. The scan frequency ranges from 10^5 to 10^{-2} Hz and the amplitude is 5 mV. The semicircular diameter in the high frequency region represents the charge transfer resistance R_{ct}, and the intersection with the real axis is the internal resistance of the electrode or the equivalent series resistance (R_s). The R_s mainly includes the contact resistance between the electrolyte solution, the current collector and the electrode material, the electrode material and the electrolyte interface, and the electrode material.

It can be seen from Figure 3 that the charge transfer resistance of Fe_3O_4 NRs/NH_2-RGO composites is 3.5 $\Omega\cdot cm^2$ and the phase angle of the middle and high frequency transition region is 45°, which reflects the response diffusion of the electrolyte in the porous electrode. The line in the low frequency region is close to 90°, indicating that the Fe_3O_4 NRs/NH_2-RGO composites electrode has ideal capacitive properties.

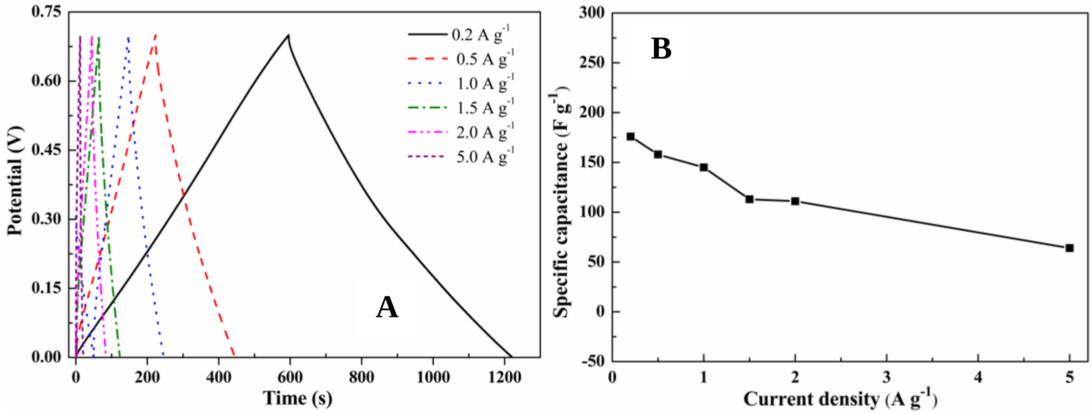

Figure 4. The galvanostatic charge-discharge curves (A) and specific capacitance (B) of the Fe_3O_4 NRs/NH_2-RGO electrode at different current densities

Charge-discharge curves and specific capacitances of Fe_3O_4 NRs/NH_2-RGO electrodes at different current densities are shown in Figure 4. Figure 4 (A) shows the charge-discharge curves of Fe_3O_4 NRs/NH_2-RGO at different current densities. The charge-discharge curves of Fe_3O_4 NRs/NH_2-RGO are symmetrical, indicating that Fe_3O_4 NRs/NH_2-RGO is energy storage by electrical double layer capacitors. With the increase of charge and discharge time the voltage linearly increases or decreases, there is no obvious platform. Figure 4 (B) shows the specific capacitance of Fe_3O_4 NRs/NH_2-RGO electrode at different current density. It was calculated that the specific capacitance 145 F/g of Fe_3O_4 NRs/NH_2-RGO at the current density of 1.0 A/g was decreased with the increase of the current density. At a high current density of 5 A/g, the specific capacitance is 92 F/g and the rate characteristic is good.

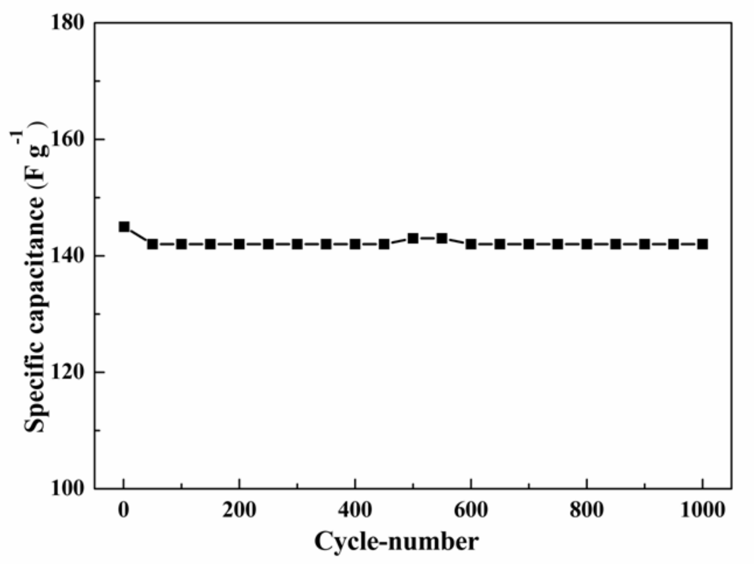

Figure 5. Cyclic stability results of Fe_3O_4 NRs/NH_2-RGO electrode at a current density of 1.0 A/g.

The cycling stability of Fe_3O_4 NRs/NH_2-RGO composites at 1.0 A/g current density is shown in Figure 5. It can be seen from Figure 5 that the specific capacitance of the Fe_3O_4 NRs/NH_2-RGO electrode is almost not attenuated after a number of cycles (the capacity retention after 1000 cycles is 99.7 %), indicating that the Fe_3O_4 NRs/NH_2-RGO electrode has a longer cycle life, showing excellent electrochemical stability. The long-term stability and retention properties of as synthesized Fe_3O_4 NRs/NH_2-RGO composites show better performance with reported articles [26, 27].

Table 1. Summary of electrochemical measurements of similar Fe_3O_4-based electrode materials in different electrolytes reported in literature.

Electrode Materials	Electrolyte	Specific Capacitance	Capacitance retention after cycle test	Ref.
Fe_3O_4/activated carbon	6 M KOH	37.9 F/g at 0.5 m/cm^2	82 % after 500 cycles	[28]
Fe_3O_4/ RGO	0.5 M Na_2SO_4	154 F/g at 1.0 A/g	97 % after 500 cycles	[29]
Fe_3O_4/RGO	1 M NaCl	151 F/g at 1.0 A/g	85 % after 1,000 cycle	[30]
Fe_3O_4/graphene nanoribbons	PVA/H_2SO_4	63.5 F/g at 1.0 A/g	95 % after 1000 cycles	[31]
Fe_3O_4 NRs/NH_2-RGO	1 M Na_2SO_4	145 F/g at 1.0 A/g	99.7 % after 1000 cycles	This work

Table 1. summarizes the literature reported performance of Fe_3O_4/Carbon-based electrode materials in different electrolytes. The Fe_3O_4 NRs/NH_2-RGO electrode shows high specific capacitance (145 F/g at 1.0 A/g) in 1 M Na_2SO_4, which even comparable with the specific capacitance of electrode materials in H_2SO_4. Moreover, the cyclic stability of Fe_3O_4 NRs/NH_2-RGO electrode of retains 99.7 % of initial capacity after 1000 cycles, which is much better than the results in literature.

4. CONCLUSIONS

In this paper, Fe_3O_4 NRs/NH_2-RGO electrode was prepared by simple hydrothermal method. The loose orientation nanostructures provide a good transport channel for the electrolyte ions, and reduce the ion in the composite during charging and discharging. The results show that the prepared electrode materials have good electrochemical activity. The prepared Fe_3O_4 NRs/NH_2-RGO electrode material reached a specific capacitance of 145 F/g at a current of 1.0 A/g, and maintained a capacity of 99.7 % after 1000 times. The results demonstrate that such Fe_3O_4 NRs/NH_2-RGO composites can be of great potential in the application of energy storage systems.

ACKNOWLEDGEMENTS
We acknowledge the financial supports of the National Natural Science Foundation of China (Grant No. 31400811).

References

1. S.K. Kim, H.J. Kim, J.C. Lee, P.V. Braun and H.S. Park, *Acs Nano*, 9 (2015) 8569-8577.
2. S.I. Kim, S.W. Kim, K. Jung, J.B. Kim and J.H. Jang, *Nano Energy*, 24 (2016) 17-24.
3. B.P. Krishnan, S. Mukherjee, P.M. Aneesh, M.A.G. Namboothiry and K.M. Sureshan, *Angew. Chem. Int. Edit.*, 55 (2016), 2345-2349.
4. K. Lee, Y. Yoon, Y. Cho, S.M. Lee, Y. Shin, H. Lee and H. Lee, *Acs Nano*, 10 **(**2016) 6799-6807.
5. W. Wang, F.H. Zhu, Y.T. Dai, H. Zhang and J.H. Lei, *Int. J. Electrochem. Sci.*, 11 (2016), 4000-4006.
6. F.W. Li, J.T. Chen, X.S. Wang, M.Q. Xue and G.F. Chen, *Adv. Funct. Mater.*, 25 (2015) 4601-4606.
7. M. Li, F. Pan, E.S.G. Choo, Y.B. Lv, Y. Chen and J.M. Xue, *Acs. Appl. Mater. Inter.*, 8 **(**2016) 6972-6981.
8. Y. H. Li, Q.Y. Li, H.Q. Wang, Y.G. Huang, X.H. Zhang, Q. Wu, H.Q. Gao and J.H. Yang, *Appl. Energ.*, 153 **(**2015) 78-86.
9. B.L. Liang, Z.Y. Qin, T. Li, Z.J. Dou, F.X. Zeng, Y.M. Cai, M.F. Zhu and Z. Zhou, *Electrochim. Acta*, 177 (2015) 335-342.
10. Z. Li, J. Liu, K.R. Jiang and T. Thundat, *Nano Energy*, 25 (2016) 161-169.
11. S. Nejati, T.E. Minford, Y.Y. Smolin and K.K.S. Lau, *Acs Nano*, 8 (2014) 5413-5422.
12. C. Mondal, D. Ghosh, T. Aditya, A.K. Sasmal and T. Pal, *New J. Chem.*, 39 **(**2015) 8373-8380.
13. J.Y. Cheng, B. Zhao, W.K. Zhang, F. Shi, G.P. Zheng, D.Q. Zhang and J.H. Yang, *Adv. Funct. Mater.*, 25 (2015) 7381-7391.
14. W. Huang, H.H. Zhong, D.Q. Li, P.G. Tang and Y.J. Feng, *Electrochim. Acta*, 173 (2015) 575-580.
15. R.Z. Li, X. Ren, F. Zhang, C. Du and J.P. Liu, *Chem. Commun.*, 48 (2012) 5010-5012.
16. X. C. Li, L. Zhang and G.H. He, *Carbon*, 99 (2016) 514-522.
17. W. Wang, P.X. Ma, H. Dong, H.J. Krause, Y. Zhang, D. Willbold, A. Offenhaeusser and Z.W. Gu, *Biosens. Bioelectron.*, 80 (2016) 661-665.
18. W. Wang, M.Y. He, H. Zhang and Y.T. Dai, *J. Magn.*, 21 (2016) 179-182.
19. W. Wang, M.Y. He, H. Zhang and Y.T. Dai, *Int. J. Electrochem. Sci.*, 11 (2016) 1831-1839.

20. L. Li, P. Gao, S.L. Gai, F. He, Y.J. Chen, M.L. Zhang and P.A.P. Yang, *Electrochim. Acta*, 190 (2016) 566-573.
21. J. Liu, S.Q. Liu, S.X. Zhuang, X.W. Wang and F.Y. Tu, *Ionics*, 19 (2013) 1255-1261.
22. C.J. Jia, L.D. Sun, F. Luo, X.D. Han, L.J. Heyderman, Z.G. Yan, C.H. Yan, K. Zheng, Z. Zhang, M. Takano, N. Hayashi, M. Eltschka, M. Klaui, U. Rudiger, T. Kasama, L. Cervera-Gontard, R.E. Dunin-Borkowski, G. Tzvetkov and J. Raabe, *J. Am. Chem. Soc.*, 130 (2008) 16968-16977.
23. W. S. Hummers and R.E. Offeman, *J. Am. Chem. Soc.*, 80 (1958) 1339-1339.
24. Q. Wu, Y. Xu, Z. Yao, A. Liu and G. Shi, *Acs Nano*, 4 (2010) 1963-1970.
25. S.D. Min, C.J. Zhao, Z.M. Zhang, G.R. Chen, X.Z. Qian, Z.P. Guo, *J. Mater. Chem. A*, 3 (2015) 3641-3650.
26. J.P. Cheng, Q.L. Shou, J.S. Wu, F. Liu, V.P. Dravid and X.B. Zhang, *J. Electroanal. Chem.*, 698 (2013) 1-8.
27. L. Li, Y. Dou, L. Wang, M. Luo, J. Liang, *RSC Adv.*, 4(2014) 25658-25665.
28. D. Xuan, W. Chengyang, C. Mingming, J. Yang and W. Jin, *J. Phys. Chem. C*, 113 (2009) 2643-2646.
29. S. Ghasemi and F. Ahmadi, *J. Power Sources*, 289 (2015), 129-137.
30. W.H. Khoh and J.D. Hong, *Colloids Surf. A: Physicochem. Eng. Aspects*, 436 (2013) 104-112.
31. S. Lalwani, V. Sahu, R.B. Marichi, G. Singh and R.K. Sharma, *Electrochim. Acta*, 224 (2017) 517-526.